

# Cavitating flow analysis and design optimization for a waterjet mixed flow pump

R F Huang<sup>1,2</sup>, Z H Zhai<sup>2</sup>, J J Zhou<sup>2</sup> and X W Luo<sup>1\*</sup>

<sup>1</sup> State Key Laboratory of Hydrosience and Engineering, Tsinghua University, Beijing 100084, China

<sup>2</sup> Science and Technology on Water Jet Propulsion Laboratory, Shanghai 200011, China

Email: luoxw@mail.tsinghua.edu.cn

**Abstract.** This research investigates cavitation flow simulation and design optimization for a waterjet mixed flow pump whose design flow coefficient is 0.183 and rotational speed is 1450 r/min. Both the hydraulic and cavitation characteristics are predicted and compared with model test. In order to improve the pump performance, an optimized impeller is obtained with the blade thickness reducing by 0.6 mm and adjusting the blade inlet angle. The cavitating flow in a waterjet mixed flow pump is simulated using the SST  $k-\omega$  turbulence model and homogeneous cavitation model with a single blade-to-blade flow passage. Compared with the experimental results, the numerical data are in reasonable agreement for predicting hydraulic characteristics and show a similar trend in cavitation performance prediction. Future work will focus on improving the cavitation model for better accuracy of cavitation prediction. Based on the experimental test and commercial software CFX simulation, it can be concluded that reducing the blade thickness and inlet angle can have favorite effects on the hydraulic performance as well as cavitation performance.

## 1. Introduction

Nowadays, more and more interest has been attracted by the waterjet propulsion which has a variety of advantages such as less vibration, low noise and high efficiency in the specified speed range <sup>[1, 2]</sup>. In recent years, the waterjet propulsion has been rapidly developed and widely used in the marine field, which is expected to be the potential technology against the propeller with the improvement in the progress of pump design, manufacture and fabrication <sup>[3]</sup>. Many scholars <sup>[4-7]</sup> have investigated the waterjet propulsion in various ships using the computational fluid dynamics (CFD) method or the model test according to the procedure proposed by the ITTC Waterjet Performance Prediction Specialist Committee <sup>[8, 9]</sup>. Kandasamy <sup>[4, 5]</sup>, Tahara <sup>[6]</sup> optimized the waterjet for high speed ships using both the simulation-based design method and model test. Bulen <sup>[7]</sup> systematically studied a waterjet propulsion system providing a reference for other researchers.

Up to now, many studies focused on the propulsion system optimization and characteristic prediction without considering cavitation in the waterjet pump. In fact, cavitation is inevitable when the waterjet pump is operated at a high speed which may result in pressure fluctuation, noise and erosion <sup>[10, 11]</sup>. Thus, good cavitation performance as well as high hydrodynamic efficiency is considered as the necessary criterion to design and evaluate a waterjet pump.



In general, experiments and numerical simulation are very useful tools to evaluate the pump performance. Until now, compared with the long-time period and huge investment of the experiment, numerical simulation has been widespread used due to the progress of computer technology, which can provide a basic understanding for the evaluation and improvement of hydraulic machines<sup>[12-15]</sup>.

In this paper, a waterjet mixed flow pump was investigated to evaluate the hydraulic performance and cavitation performance using the steady simulation with a blade-to-blade flow passage proposed by Luo<sup>[16]</sup>. The simulated data of the pump performance were compared with the available experimental data. Finally, based on the analysis of the internal flow, the waterjet pump was optimized to get better performance.

## 2. Test pump geometry

The waterjet mixed flow pump for model test consists of 6-blade impeller, 7-blade diffuser, inlet flow channel and outlet flow channel, which is designed to be operated under the following condition: flow coefficient is 0.183, and the rotational speed is 1450 r/min.

The meridional schematic diagram for the waterjet pump is shown in Figure 1, and the geometrical parameters are listed in table 1. The Reynolds number, i.e.  $Re$ , is  $2.47 \times 10^6$ , where the diameter of the impeller is taken as the specific diameter and the velocity at the inlet is taken as the specific velocity. The blade tip clearance relative to the impeller diameter is  $0.86 \times 10^{-3}$ .

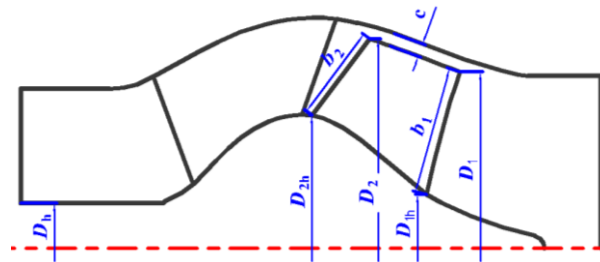


**Figure 1.** Meridional schematic diagram for the pump.

**Table 1.** Geometrical parameters for the impeller.

| Parameters                      | Symbols      | Values    |
|---------------------------------|--------------|-----------|
| Blade width ratio at the inlet  | $b_1/D_2$    | 0.318     |
| Blade width ratio at the exit   | $b_2/D_2$    | 0.247     |
| Blade inlet diameter at the tip | $D_1/D_2$    | 0.856     |
| Blade inlet diameter at the hub | $D_{1h}/D_2$ | 0.245     |
| Blade exit diameter at the hub  | $D_{2h}/D_2$ | 0.604     |
| Hub ratio                       | $D_h/D_2$    | 0.209     |
| Blade tip clearance             | $c/D_2$      | $0.86e-3$ |

## 3. Numerical method

### 3.1. Governing equations and turbulence model

A homogenous assumption is used to solve the cavitation flow, considering the liquid and vapor flow as a single one and sharing the same velocity and pressure fluid. Assuming the liquid and vapor phases incompressible, the mixture flow can be described by the Reynolds Averaged Navier-Stokes (RANS) equations as follows:

$$\frac{\partial \rho_m}{\partial t} + \frac{\partial}{\partial x_j} (\rho_m u_j) = 0 \quad (1)$$

$$\frac{\partial}{\partial t}(\rho_m u_i) + \frac{\partial}{\partial x_j}(\rho_m u_i u_j) = -\frac{\partial p}{\partial x_i} + \mu_m \frac{\partial^2 u_i}{\partial x_j \partial x_j} - \frac{\partial}{\partial x_j}(\rho_m \overline{u'_i u'_j}) \quad (2)$$

$$\frac{\partial \rho_v \alpha_v}{\partial t} + \nabla \cdot (\rho_v \alpha_v \mathbf{u}) = \dot{m}_e^+ - \dot{m}_c^- \quad (3)$$

where the  $\rho_m$ ,  $\mu_m$  are density and dynamic viscosity of the homogenous phase;  $p$ ,  $u$  are the pressure and velocity;  $\rho_v$ ,  $\alpha_v$  respectively represent the vapor phase density and volume fraction. The source terms  $\dot{m}_e^+$  and  $\dot{m}_c^-$  are derived from the cavitation model.

The mixture density  $\rho_m$  and the mixture dynamic viscosity  $\mu_m$  are defined as follows:

$$\rho_m = \alpha_v \rho_v + (1 - \alpha_v) \rho_l \quad (4)$$

$$\mu_m = \alpha_v \mu_v + (1 - \alpha_v) \mu_l \quad (5)$$

where subscript v, l represent the vapor and liquid respectively.

In this research, the  $k-\omega$  SST model is adopted to obtain highly accurate predictions of flow separation under adverse pressure gradients because this turbulence model accounts for the transport of the turbulent shear stress.

### 3.2. Cavitation model

The cavitation model developed by Zwart [17] is proposed to solve the vapour volume fraction  $\alpha_v$  in equation (3). Then, the Rayleigh-Plesset equation is applied to solve the source terms  $\dot{m}_e^+$  and  $\dot{m}_c^-$  controlling vapour generation and condensation.

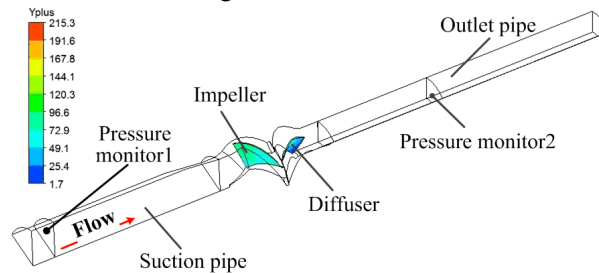
$$\dot{m}_e^+ = F_{\text{vap}} \frac{3r_{\text{nuc}}(1 - \alpha_v)\rho_v}{R_{\text{nuc}}} \sqrt{\frac{2}{3} \frac{\max(p_v - p, 0)}{\rho_l}} \quad (6)$$

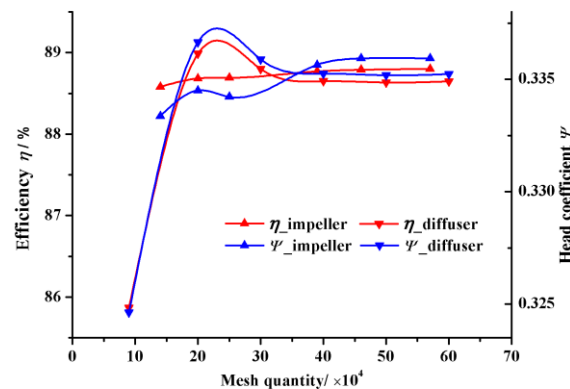
$$\dot{m}_c^- = F_{\text{cond}} \frac{3\alpha_v \rho_v}{R_{\text{nuc}}} \sqrt{\frac{2}{3} \frac{\max(p - p_v, 0)}{\rho_l}} \quad (7)$$

To obtain the interphase mass transfer rate, four model parameters are given as follows: bubble radius  $R_{\text{nuc}} = 1 \mu\text{m}$ , the nucleation volume fraction  $r_{\text{nuc}} = 5\text{E-}4$ , the evaporation coefficient  $F_{\text{vap}} = 50$  and the condensation coefficient  $F_{\text{cond}} = 0.01$ .

### 3.3. Mesh generation and mesh independence test

The computational domain is divided into the suction pipe, the outlet pipe, the impeller and the diffuser. Two interfaces are set in the suction and outlet pipe to monitor the total pressure. The structured hexahedral mesh is applied to obtain accurate simulation results. The topological structure and mesh point distribution are the same in different models. What is more, mesh around the impeller blade and diffuser blade are refined to satisfy the requirement for the turbulence model with the  $Y_{\text{plus}}$  less than 121 in most regions as shown in figure 2.



**Figure 2.** Computation domain and Yplus distribution.**Figure 3.** Mesh independence test.

In order to exclude the effect of mesh on the prediction accuracy, the impeller and diffuser is gradually increasing mesh density to test its independence and the pump characteristics such as head coefficient and efficiency are calculated as independence criterions as shown in figure 3. It can be concluded that the pump head coefficient and efficiency are more sensitive to mesh density in diffuser than that in impeller. When the mesh quantity in impeller and diffuser reach 400,000 respectively, the pump head coefficient and efficiency remain unchanged. Considering the calculation resource, the mesh quantity is decided to be 460,000 in impeller and 400,000 in diffuser as marked in figure 3. The mesh quality is evaluated by the determinant  $2 \times 2 \times 2$ , which is more than 0.395 in the impeller and more than 0.584 in the diffuser.

### 3.4. Computational method

The CFD code ANSYS CFX 14.0 is used to solve the RANS equations. With automatic wall function, the  $k-\omega$  SST turbulence model is applied to simulate the steady turbulent flow in the waterjet pump. High resolution scheme is set for the advection term and the turbulence numeric.

The impeller is a rotating part and other parts are static, therefore, the multiple reference frame (MRF) is used in this simulation and interface between the rotating part and static parts is set to be frozen-rotor under steady condition.

For boundary conditions, the mass flow rate is given at the outlet plane based on the mass equilibrium and one – seventh of the total mass flow is set because the flow passage is single blade-to-blade. The total pressure is applied at the inlet plane and gradually reducing when cavitation occurs. All solid walls are set as the non-slip wall condition.

## 4. Results and discussions

### 4.1. Numerical analysis method and its validation

The calculated and experimental results of the waterjet mixed flow pump are presented using non-dimensional parameters listed in table 2.

**Table 2.** Non-dimensional parameters

| Definition                | Symbol      | Expression                                |
|---------------------------|-------------|---|
| Head coefficient          | $\Psi$      | $\frac{H}{u_2^2/2g}$                      |
| Flow coefficient          | $\phi$      | $\frac{Q}{\pi D_2 b_2 u_2}$               |
| Input power coefficient   | $\tau_{in}$ | $\frac{P_{in}}{\rho \pi D_2 b_2 u_2^3/2}$ |
| cavitation specific speed | $c$         | $\frac{5.62n\sqrt{Q}}{NPSH_c^{3/4}}$      |

The comparison of hydrodynamic characteristics of model A is shown in figure 4 under different operation conditions and in figure 5 at design condition. It is noted that model A is conducted using both experimental (marked as exp.) and numerical (marked as cal.) methods. As can be seen from figure 4, the numerical data of pump head coefficient for model A agree well with the experimental data while there is a difference in the axial input power coefficient between the calculated and experimental data because there are some loss in actual pump segment which cannot be accurately computed. Therefore, the numerical efficiency for model A is higher than the experimental one reasonably.

Net Positive Suction Head (*NPSH*) is usually used to describe the cavitation characteristics in pumps whose expression is shown subsequently:

$$NPSH = \left( \frac{p_t}{\rho_l g} - H_g - h_w \right) - \frac{p_v}{\rho_l g} \quad (8)$$

where  $p_t$  is the total pressure at the inlet monitored plane as shown in Figure 2;  $H_g$  is the geometrical installation height which can be ignored to a waterjet pump;  $h_w$  is hydraulic loss which is considered to be zero in this study.

To be convenient for comparison, the Thoma's cavitation number, i.e.  $\sigma_t$ , is recommended as follows:

$$\sigma_t = \frac{NPSH}{H} \quad (9)$$

where  $H$  is the pump head at the best efficiency point with the designed flow rate.

The critical *NPSH*, i.e., *NPSH<sub>c</sub>*, is defined as the *NPSH* value when the pump head drops 3% from its original value at the designed point. Therefore, the cavitation specific speed can be worked out using the equation in table 2.

Figure 6 shows the cavitation characteristics by simulation and experiments. The  $\sigma_t$  for calculated method is 0.36 and for experimental method is 0.49. The cavitation specific speed for simulation is 1876 and for experiments is 1505. There is a difference in cavitation specific speed between simulation and experiments because many factors in the real model test such as gas in local water and water temperature can't be taken into account during the simulation. Thus, the results are reasonable and within the range of tolerance. Therefore, it can be concluded that calculated results by CFX code are reliable to investigate the hydraulic and cavitation characteristics of the waterjet mixed-flow pump.

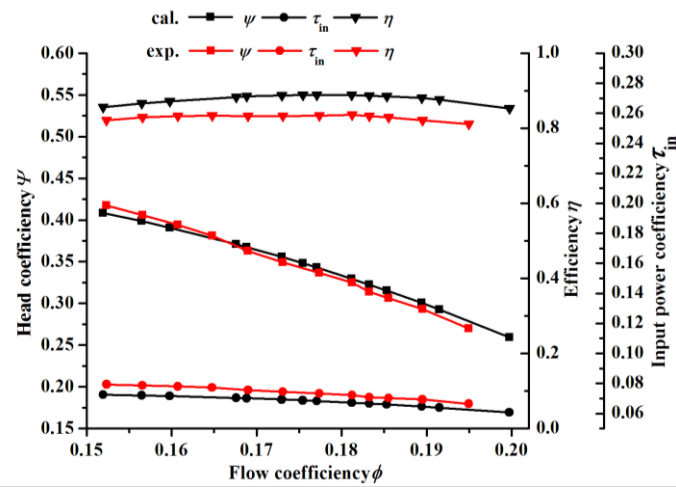


**Figure 4.** Hydrodynamic characteristic curves of model A.

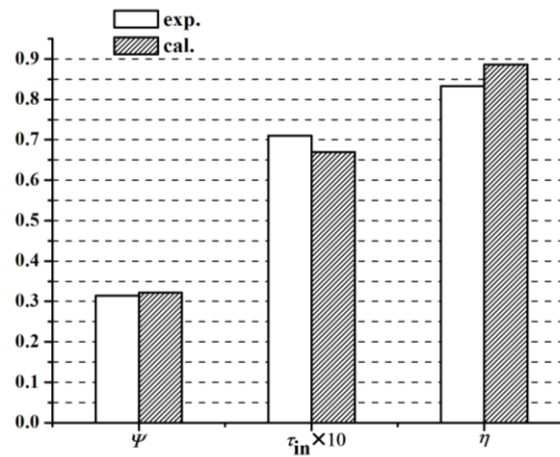


**Figure 5.** Hydrodynamic characteristic comparison at design condition of model A.

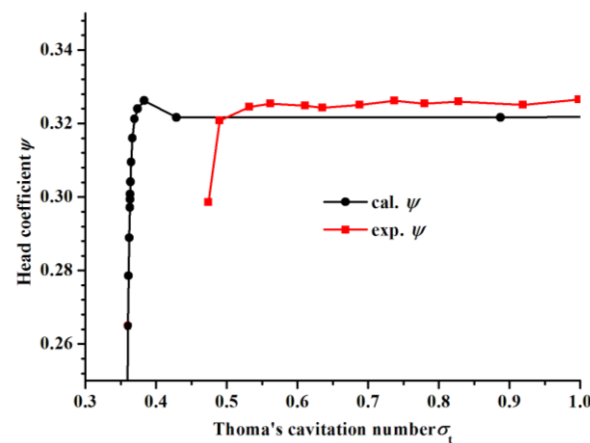


**Figure 6.** Cavitation characteristics of model A for numerical method and experimental method.

#### 4.2. Design optimization and analysis

For the first design stage, the pump is required to reach efficiency as high as possible and its cavitation specific speed is strictly requested higher than 1300 for its application as a waterjet pump. To achieve better hydrodynamic performance, based on the experimental and computational data for the model A pump, an optimized waterjet pump named as model B is built. The blade thickness of model B pump is reduced by 0.6 mm and the leading edge transits smoothly with larger ellipse, and then the blade inlet angle is adjusted because there is triangular low-pressure area in the suction side.

Figure 7 shows the hydraulic characteristics of model A and model B operated at design condition. Both head coefficient and efficiency of model B is higher than that of model A. Based on the static pressure and velocity distribution on the suction side shown in figure 8, it can be noted that reducing blade inlet angle can make the triangular low-pressure area smaller. The velocity close to hub in model A flows towards shroud which may flow separation, but this bad flow patterns are improved in model B.

Figure 9 shows the cavitation characteristics of the two models operated at design condition and the Thoma's cavitation number is 0.3473 when there is deep cavitation in the impeller demonstrated from Figure 6. Both head coefficient and efficiency of model B performs better than model A under deep cavitation condition.

The Boundary Vorticity Flux (BVF) [18] is used to analyse the internal flow as shown in figure 10. The BVF definition for the incompressible fluid is as follows:

$$\zeta = \frac{\partial(\mu\Omega)}{\partial n} = n \bullet \nabla(\mu\Omega) \quad (10)$$

where  $n$  is the normal direction of the local wall and  $\Omega$  corresponds to the local absolute vorticity.

BVF is contributed by the accelerated speed, the pressure gradient and the boundary vorticity, but the pressure gradient is the only working one in the hydraulic rotation machineries, demonstrated by Zhang [19, 20]. Finally, the BVF is denoted as:

$$\zeta = \frac{n_z}{\rho} \times \nabla p \quad (11)$$

BVF peak is shown at the leading edge for the waterjet model A pump, demonstrating that it is possible to have flow separation in those areas. However, the peak area in model B is cut off obviously. There are bands with positive or negative BVF values alternatively on the impeller suction side, which means that the pressure gradient is turned around, resulting in unfavourable effects on the internal flow, but this phenomenon is improved in model B.

Vapour volume fraction at three spans of the impeller shown in figure 11 illustrates cavitation patterns in the waterjet mixed-flow pump. The blue colour represents water and red represents vapour cavities. It can be noted that cavities are likely to generate on the suction side and then grow up from leading edge to tailing edge. However, there are a lot more cavities at mid-span of model A than that of model B which affects the static pressure distribution along the impeller. The horizontal data in figure 12 demonstrate that local pressure is under saturation pressure and cavities generate in those area which is in good agreement with the vapour fraction distribution shown in figure 11. In addition, the static pressure in the optimized model B is higher than that in model A which demonstrates that model B performs better efficiency.



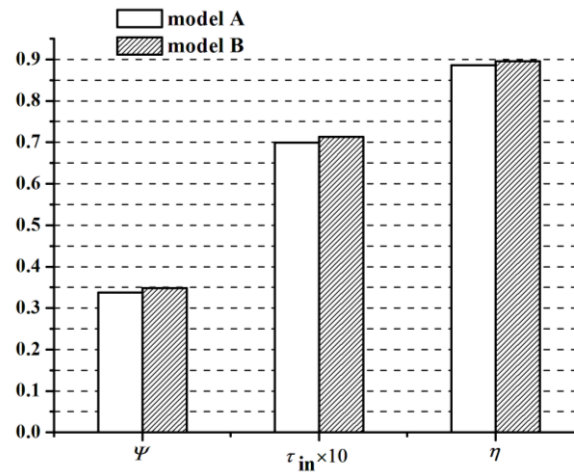


**Figure 7.** Hydraulic characteristics at design operation condition ( $\phi=0.183$ ,  $n=1450$  r/min).

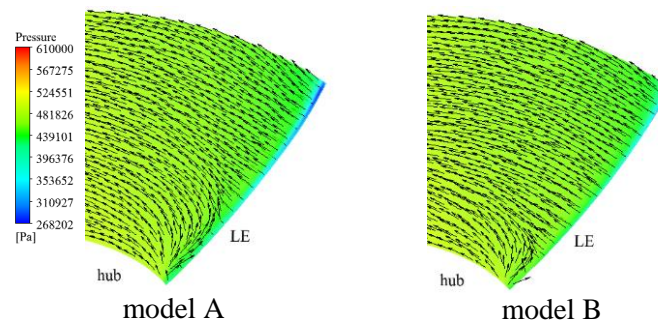


**Figure 8.** Static pressure and velocity distribution on the suction side under design operation condition (left-model A; right-model B).

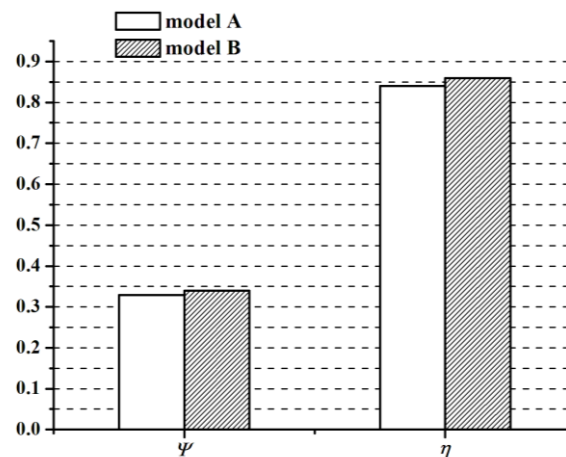


**Figure 9.** Cavitation characteristics at design operation condition ( $\phi=0.183$ ,  $n=1450$  r/min,  $\sigma_t=0.3473$ ).



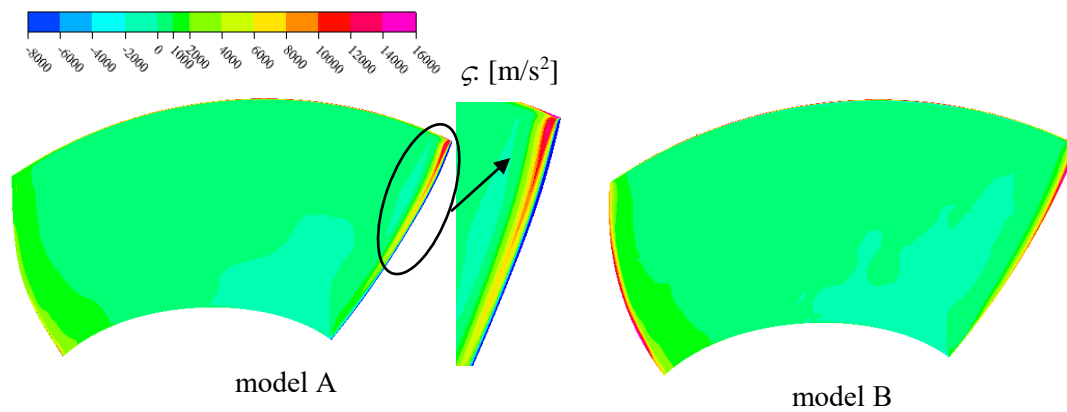


**Figure 10.**  $\zeta$  distribution on the suction side under design operation condition.

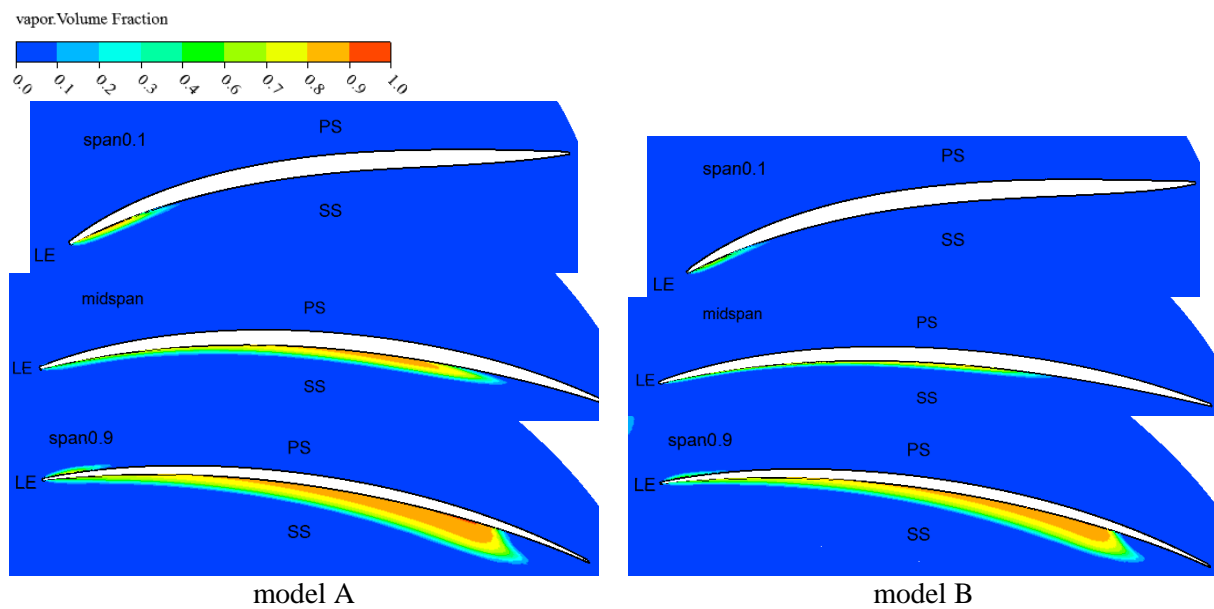


**Figure 11.** Vapor volume fraction at three spans of the impeller.

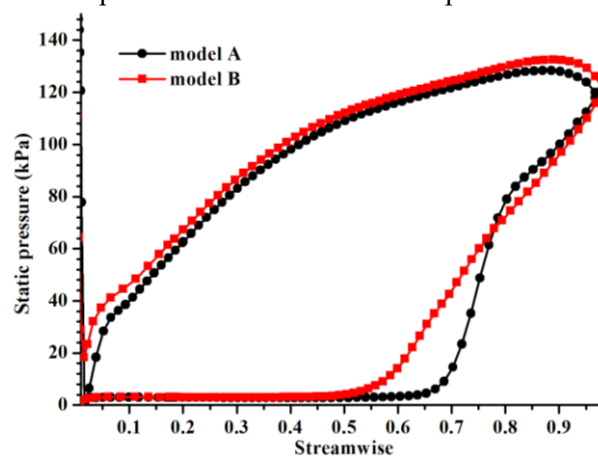


**Figure 12.** Static pressure distribution at mid-span of the impeller.

## 5. Conclusions

In this paper, the hydraulic performance and cavitating flow behaviour in a waterjet mixed flow pump have been studied by numerical and experimental methods under various conditions. Based on the above results and discussions, several conclusions can be drawn:

Based on the RANS, the SST  $k-\omega$  turbulence model is used to predict the hydraulic performance in noncavitating conditions and results show reasonable agreement with the experimental results, although the calculated efficiency is always lower than the experimental efficiency without considering hydraulic loss.

Homogeneous cavitation model is applied to predict the cavitation evolution in the waterjet pump and the simulated results show the similar trend to the experimental data. Future work will focus on improving the cavitation model considering turbulence interaction to reduce the tolerance error.

After analysing the experimental and simulated data, an optimized waterjet pump is built with the blade thickness reducing by 0.6 mm and adjusting the blade inlet angle. Based on the CFX code simulation results, it can be concluded that reducing the blade thickness and inlet angle can have favourable effects on the hydraulic performance as well as cavitation performance.

## Acknowledgments

This work was financially supported by National Natural Science Foundation of China (Project Nos. 51376100 and 51776102), the State Key Laboratory for Hydrosience and Engineering (Project No. 2017-E-02) and Tsinghua National Laboratory for Information Science and Technology.

## References

- [1] Kandasamy M, He W, Takai T, Tahara Y, Peri D, Campana E, Wilson W and Stern F 2011 Opti-mization of waterjet propelled high speed ships—JHSS and Delft Catamaran Proc. FAST11 (Hawaii, USA)
- [2] Carlton J 2012 Marine propellers and propulsion (Oxford, Butterworth-Heinemann)
- [3] Takai T, Kandasamy M and Stern F 2011 Verification and validation study of URANS simulations for an axial waterjet propelled large high-speed ship J. Mar. Sci. Technol. 16 (4) 434-447
- [4] Kandasamy M, Peri D, Tahara Y, Wilson W, Miozzi M, Georgiev S, Milanov E, Campana E and Stern F 2013 Simulation based design optimization of waterjet propelled Delft catamaran Int. Ship-building Progress 60 (1) 277-308
- [5] Kandasamy M, Georgiev S, Milanov E and Stern F 2011 Numerical and experimental evaluation of waterjet propelled delft catamarans Proc. FAST11 (Hawaii, USA)
- [6] Tahara Y, Hino T, Kandasamy M, He W and Stern F 2011 CFD-based multiobjective optimization of waterjet propelled high speed ships Proc. FAST11 (Hawaii, USA)
- [7] Bulten N W H 2006 Numerical analysis of a waterjet propulsion system (Eindhoven University of Technology)
- [8] Van T T 2005 Report of the specialist committee on validation of waterjet test procedures Proc. ITTC24 471-508
- [9] Kim K, Turnock S R, Ando J, Becchi P, Korkut E, Minchew A, Semionicheva E Y, Van S H and Zhou W X 2008 The propulsion committee: final report and recommendations to the 25th ITTC Proc. ITTC25
- [10] Yu A, Yu W P, Pan Z B, Luo X W, Ji B and Xu H Y 2013 Cavitation performance evaluation for a condensate pump IOP Conf. Ser.: Mater. Sci. Eng. 52 (6) 062014
- [11] Luo X W, Ji B and Xu H Y 2012 Design and op-timization for fluid machinery (Beijing: Tsinghua University Press)
- [12] Luo X W, Zhang Y, Peng J Q, Xu H Y and Yu W P 2007 Impeller inlet geometry effect on performance improvement for centrifugal pumps J. Mech. Sci. Tech. 22 (10) 1971-1976

- [13] Ji B, Luo X W, Wang X, Peng X X, Wu Y L and Xu H Y 2011 Unsteady numerical simulation of cavitating turbulent flow around a highly skewed model marine propeller *J. Fluids Eng.* 133 (1) 011102
- [14] Luo X W, Zhang Y, Peng J Q and Xu H Y 2008 Effect of impeller inlet geometry on centrifugal pump cavitation performance *Tsinghua Sci. Tech.* 05 836-839
- [15] Ji B, Luo X W, Peng X X, Wu Y L and Xu H Y 2012 Numerical analysis of cavitation evolution and excited pressure fluctuation around a propeller in non-uniform wake *Int. J. Multiphase Flow* 43 13-21
- [16] Luo X W, Wei W, Ji B, Pan Z B, Zhou W C and Xu H Y 2013 Comparison of cavitation prediction for a centrifugal pump with or without volute casing *J. Mech. Sci. Tech.* 27 (6) 1643-1648
- [17] Zwart P J, Gerber A G and Belamri T 2004 A two-phase flow model for predicting cavitation dynamics *Pro. Int. Conf. Multiphase Flow (Yokohama, Japan)*
- [18] Wu J, Ma H and Zhou M 2006 *Vorticity and vortex dynamics* (Germany: Springer)
- [19] Zhang R and Chen H 2012 Numerical simulation and flow diagnosis of axial-flow pump at part load condition *Int. J. Turbo Jet* 29 (1) 1-7
- [20] Zhang R and Chen H 2013 Numerical analysis of cavitation within slanted axial-flow pump *J. Hydrodynamics* 25 (5) 663-672